



# Evolutions of Oil Generation and Expulsion of Marine-Terrestrial Transitional Shales: Implications From a Pyrolysis Experiment on Water-Saturated Shale Plunger Samples

Qizhang Fan<sup>1,2</sup>, Peng Cheng<sup>2,3\*</sup>, Xianming Xiao<sup>1</sup>, Haifeng Gai<sup>2,3</sup>, Qin Zhou<sup>2,3</sup>, Tengfei Li<sup>2,3</sup> and Ping Gao<sup>1</sup>

## OPEN ACCESS

### Edited by:

Kai-Jun Zhang,  
University of Chinese Academy of  
Sciences, China

### Reviewed by:

Yang Wang,  
China University of Mining and  
Technology, China  
Hongxiang Guan,  
Ocean University of China, China

### \*Correspondence:

Peng Cheng  
chengp@gig.ac.cn

### Specialty section:

This article was submitted to  
Geochemistry,  
a section of the journal  
Frontiers in Earth Science

**Received:** 30 September 2021

**Accepted:** 23 November 2021

**Published:** 24 December 2021

### Citation:

Fan Q, Cheng P, Xiao X, Gai H, Zhou Q,  
Li T and Gao P (2021) Evolutions of Oil  
Generation and Expulsion of Marine-  
Terrestrial Transitional Shales:  
Implications From a Pyrolysis  
Experiment on Water-Saturated Shale  
Plunger Samples.  
Front. Earth Sci. 9:786667.  
doi: 10.3389/feart.2021.786667

<sup>1</sup>School of Energy Resources, China University of Geosciences (Beijing), Beijing, China, <sup>2</sup>State Key Laboratory of Organic Geochemistry, Guangzhou Institute of Geochemistry, Chinese Academy of Sciences, Guangzhou, China, <sup>3</sup>CAS Center for Excellence in Deep Earth Science, Guangzhou, China

Shale reservoirs are characterized by self-generation and self-accumulation, and the oil generation and expulsion evolution model of organic-rich shales is one of important factors that obviously influence the enrichment and accumulation of shale oil and gas resources. At present, however, relevant studies on marine-terrestrial transitional shales are inadequate. In this study, a pyrolysis experiment was performed on water-saturated marine-terrestrial transitional shale plunger samples with type II<sub>b</sub> kerogen to simulate the evolutions of oil generation and expulsion. The results indicate that marine-terrestrial transitional shales have wider maturity ranges of oil generation and expulsion than marine and lacustrine shales, and the main stages of oil expulsion are later than those of oil generation, with corresponding R<sub>o</sub> values of 0.85%–1.15% and 0.70%–0.95%, respectively. Although the oil generation and expulsion process induced a fractionation in compositions between the expelled and retained oils, both the expelled and retained oils of marine-terrestrial transitional shales are dominated by heavy compositions (resins and asphaltenes), which significantly differs from those of marine and lacustrine shales. The kerogen of marine-terrestrial transitional shales initially depolymerized to transitional asphaltenes, which further cracked into hydrocarbons, and the weak swelling effects of the kerogen promoted oil expulsions. The oil generation and expulsion evolutions of these shales are largely determined by their organic sources of terrigenous higher organisms. This study provides a preliminary theoretical basis to reveal the enrichment mechanism of marine-terrestrial transitional shale oil and gas resources.

**Keywords:** marine-terrestrial transitional shale, pyrolysis experiment, oil generation and expulsion, organic sources, maturity

## INTRODUCTION

Organic-rich shales are widely developed in marine, lacustrine, and marine-terrestrial transitional strata in China, and the three types of shales significantly contributed to the oil and gas resources of both conventional and unconventional reservoirs (Zou et al., 2019; Zou et al., 2020). In the Sichuan Basin, for example, giant gas fields in the central Sichuan Basin, including the Anyue, Weiyuan, and Ziyang shale gas plays, were mainly sourced from the Lower Paleozoic marine shales (Zou et al., 2014); several tight sandstone gas reservoirs in the paleo-uplift of the central Sichuan Basin largely came from the Jurassic lacustrine shales (Huang et al., 2019); the Xinchang gas field in the western Sichuan Basin were basically derived from the Upper Triassic marine-terrestrial transitional shales (Chen et al., 2010; Wu et al., 2016). In the last 2 decades, developments of marine shale oil and gas resources in the North America have achieved a great success (Zhou et al., 2019). Marine shale gases and lacustrine shale oils in China also have been commercially developed in the past 10 years (Jin et al., 2019; Zhao et al., 2020). Although marine-terrestrial transitional shales were believed to have a large potential of shale oil and gas resources, few of them have achieved commercial developments until now (Guo et al., 2015; Guo et al., 2021).

Marine-terrestrial transitional source rocks generally have low yields of oil generation, and most of the generated oils remained in source rocks (Liu et al., 2005; Mao et al., 2012). Therefore, these source rocks are commonly believed to have few contributions to normal petroleum reservoirs. However, the oil and gas resources of marine-terrestrial transitional shale reservoirs are largely determined by their oil generation and expulsion model because shale strata generally acted as both source rocks and reservoirs. Although oil generation and expulsion models have been well documented for marine and lacustrine shales in many previous studies (Wei et al., 2012; Han et al., 2015; Tang et al., 2015; Han et al., 2017; Ziegs et al., 2017; Hakimi et al., 2018; Wu et al., 2018), relevant studies on marine-terrestrial transitional shales are still inadequate presently. Marine-terrestrial transitional shales generally have thin single layers and thick cumulative thickness. The sedimentary facies of marine-terrestrial transitional shales vary obviously with burial depth resulting in their organic and inorganic compositions exhibiting obvious heterogeneity, and these shales are obviously richer in terrestrial organic sources than the marine and lacustrine shales (Qin et al., 2016; Su et al., 2016). Because marine-terrestrial transitional shales are quite different from marine and lacustrine shales in both geological and geochemical characteristics, the oil generation and expulsion models deduced from the latter shales failed to be applied on the former shales. At present, oil generation and expulsion characteristics of marine-terrestrial transitional shales are still not fully understood, which limits the development of their oil and gas resources.

In previous studies, dried shale powder samples were commonly used for pyrolysis experiments (Inan and Schenk, 2001; Carr et al., 2009; Liang et al., 2015; Ko et al.,

2018). However, this method has several disadvantages to simulate oil generation and expulsion of shale samples. Shale pore structures, especially the microfractures, may be obviously broken during crushing process, which affects the expulsion and storage of generated shale oils. In addition, connate pore waters in source rocks significantly influence oil generation process and the properties of generated oils (Sun et al., 2015). For example, artificially simulated oils generated under water-bearing conditions are more similar with natural oil samples than those generated under anhydrous conditions (Lewan et al., 1979). Differing from the methods in previous studies, in this study, small shale plunger samples that drilled from a lowly mature marine-terrestrial transitional shale core sample were first saturated with water, and then they were used for a pyrolysis experiment to simulate the oil generation and expulsion characteristics. This study intends to provide a preliminary theoretical model to further reveal the enrichment mechanism of marine-terrestrial transitional shale oil and gas resources.

## EXPERIMENTS

### Pyrolysis Experiments

In this study, water-saturated shale plunger samples were used for the pyrolysis experiment performed in gold tube reactors (Tang et al., 2005; Tian et al., 2012; Gai et al., 2015; Ko et al., 2018). The main experimental procedures are as follows: small shale plunger samples (30 mm in height × 8 mm in diameter) were drilled from the inner part of a big shale core sample in vertical stratification direction. After they were dried in an oven at 105°C for 24 h, the shale plunger samples were saturated with deionized water in a BH-1 pressurized instrument (Cheng et al., 2019). Then, the water-saturate shale plungers were loaded in gold tubes (70 mm length × 9 mm inside diameter), and both sides of the gold tube were filled with quartz sands to collect expelled oils. Next, the gold tubes were separately loaded into pressure vessels in a high-temperature high-pressure pyrolysis oven. The given temperatures of this experiment were 350°C, 375°C, 395°C, 415°C, 435°C, and 460°C, respectively. During the experiment, the pyrolysis instrument was heated at a rate of 20°C/h, and the experimental pressure was maintained approximately 50 MPa (±1 MPa).

### TOC and Mineralogical Analysis

Shale samples were powdered to a grain size of less than 180 μm and were eluted by diluted hydrochloric acids to remove the carbonates. After the shale powders were dried in an oven, their TOC contents were analyzed by an Eario El Cube Elemental Analyzer. The analytical errors of the instrument is less than 0.1%. The mineralogical compositions of shales were analyzed by a Bruker D8 Advance x-ray diffractometer. The measurements were performed on shale grains less than 75 μm at 40 kV and 30 mA with Cu Kα radiation. The relative content of minerals was semi-quantitatively calculated based on their

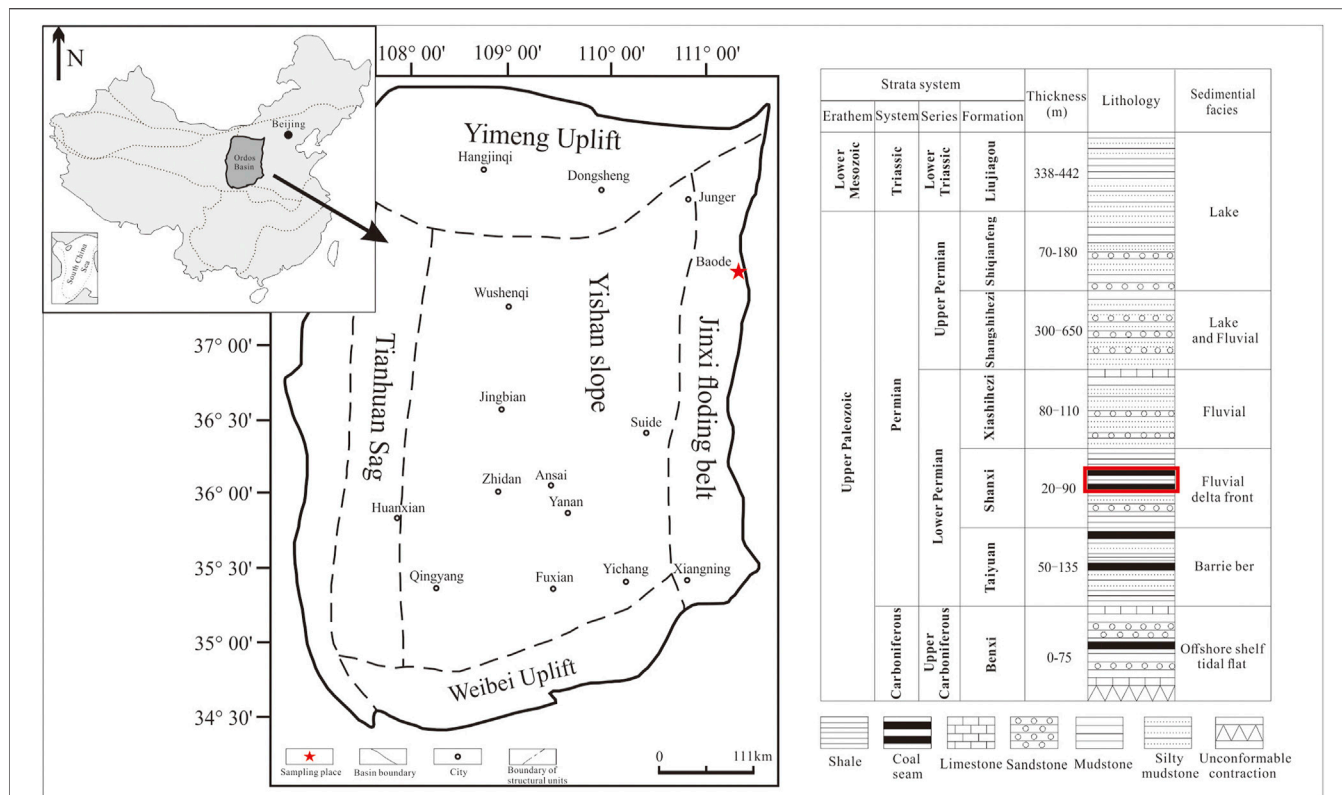


FIGURE 1 | Schematic maps showing the location and stratum of the studied shale sample (modified after Cao et al., 2019 and Su et al., 2005).

TABLE 1 | Geological and geochemical data of the shale sample used for pyrolysis experiment in this study.

Sample	Region	Stratum	Lithology	TOC (%)	R <sub>o</sub> (%)	Rock-eval			Mineral compositions (%)						
						T <sub>max</sub> (°C)	HI (mg/g TOC)	OI (mg/g TOC)	Quart	Clay	Pyrite	Siderite	Feldspar	Anatase	Dolomite
BLG14	Ordos Basin	Lower Permian Shanxi Formation	Black shale	15.65	0.68	434	292	2	33.6	47.5	13.6	1.5	1.3	1.6	0.9

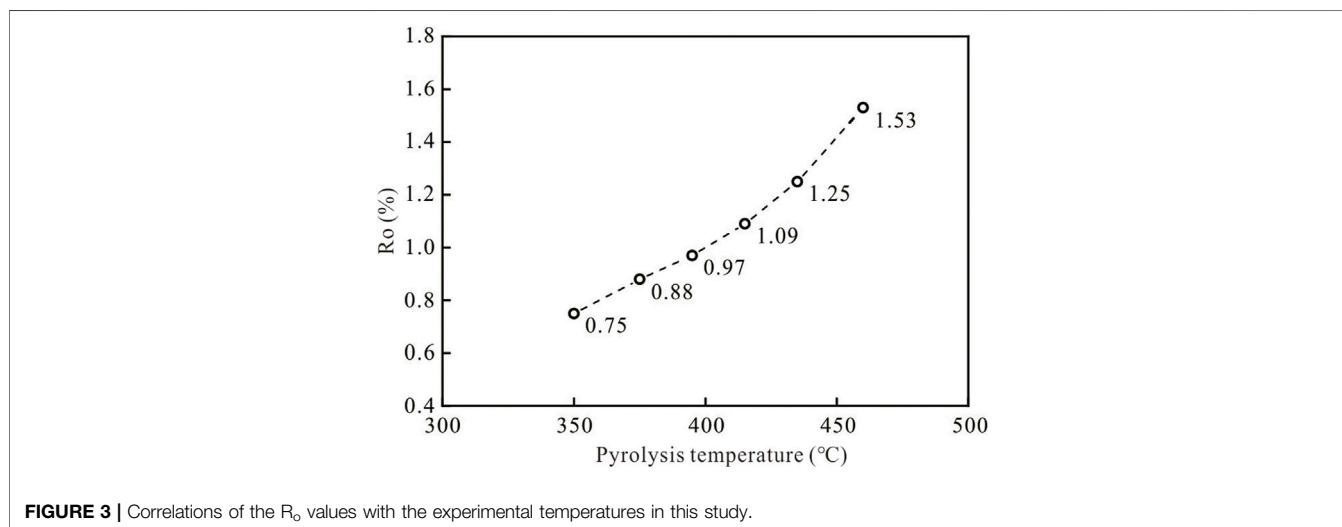
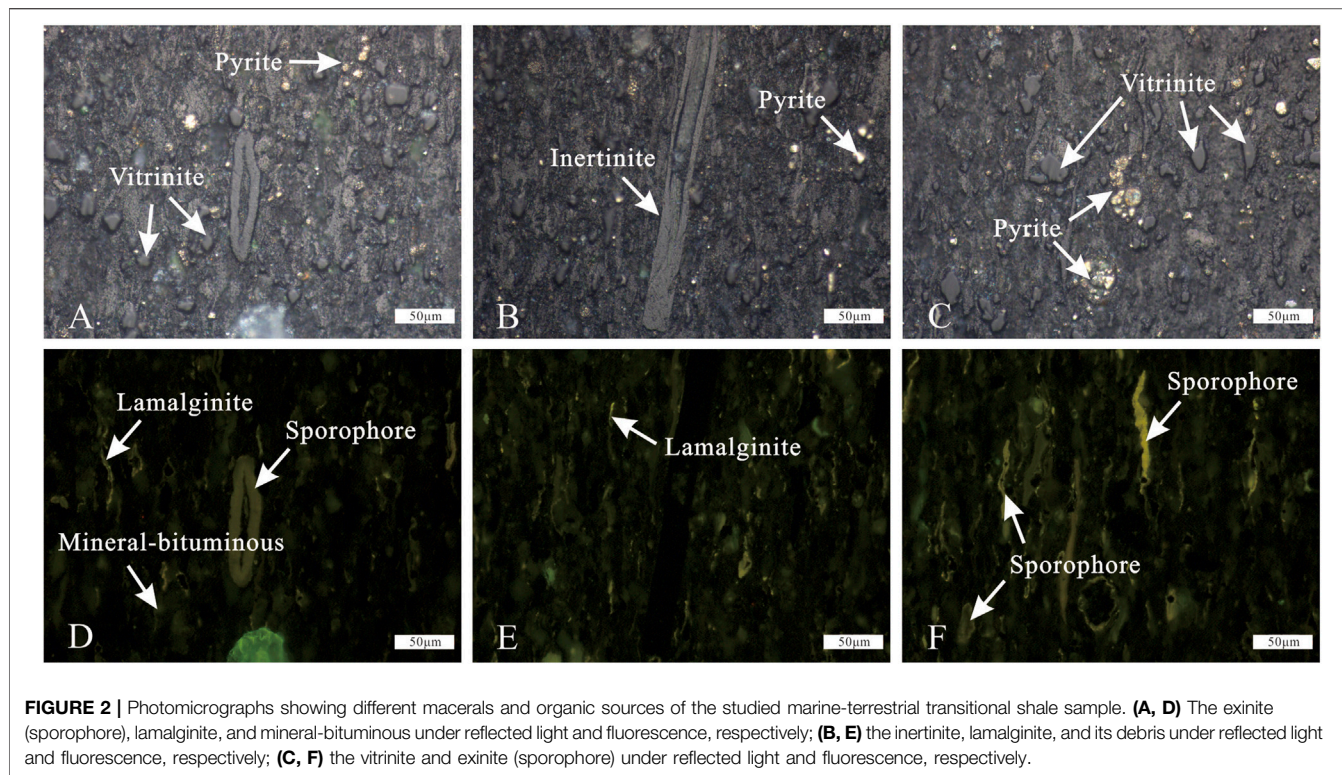
peak areas and was corrected with Lorentz-Polarization method (Chalmers and Bustin, 2008).

### Measurement of Vitrinite Reflectance (R<sub>o</sub>)

The R<sub>o</sub> values of shale samples were measured by a 3Y-DMR microphotometer equipped with a Leica microscope. The light source of this instrument is a high-pressure mercury vapor lamp with an excitation filter of 420–490 nm, and an oil immersion objective 50/1.0 is used for the measurement. Before the measurements, the instrument was calibrated by a standard yttrium aluminum garnet sample (YAG-08–57). A total of 50 individual vitrinite particles was measured for each shale sample, and the average value of these measured R<sub>o</sub> values was used in this study.

### Collection and Pretreatment of Liquid Hydrocarbons

After the pyrolysis experiment, shale plunger samples and quartz in the gold tube were separated. The shale plunger samples were crushed to powders less than 80 mesh, and then they were extracted with dichloromethane to obtain the retained oils. The collected quartz and gold tube were extracted together with dichloromethane to obtain the expelled oils. Both the retained and expelled oils were weighted by a Sartorius electronic balance with an analytical precision of 0.01 mg. The sum of the expelled and retained oils was the total generated oils. The gross compositions of these oil samples were further separated into four fractions, including saturates, aromatics,



resins, and asphaltenes, by a liquid chromatography on silica columns (Tang et al., 2005).

## RESULTS AND DISCUSSION

### Geological and Geochemical Characteristics of the Studied Shale

The shale sample used for the pyrolysis experiment was collected from the marine-terrestrial transitional strata of the Lower

Permian Shanxi Formation in the northeast of the Ordos Basin (Figure 1). It has a low maturity with a R<sub>o</sub> value of 0.68% and a high TOC content of 15.65%. The kerogen type of the shale belongs to type II<sub>b</sub> based on the van Krevelen diagram (van Krevelen, 1961), and its HI and OI values are 292 mg/g TOC and 2 mg/g TOC, respectively. The minerals of this shale mainly include clays and quartz, with contents of 47.5% and 33.6%, respectively (Table 1).

Organic petrology analysis shows that this shale sample has various macerals. It contains plenty of vitrinite and inertinite that

**TABLE 2** | Yields of the expelled oil, retained oil, and total oil for the studied marine-terrestrial transitional shale sample at different maturity stages.

Sample number	$R_o$ (%)	Retained oil		Expelled oil		Total oil		Percentage of retained oil (%) <sup>a</sup>	Percentage of expelled oil (%) <sup>b</sup>
		(mg/g rock)	(mg/g TOC)	(mg/g rock)	(mg/g TOC)	(mg/g rock)	(mg/g TOC)		
BLG14-1	0.75	6.92	44.22	1.07	6.84	8.00	51.12	86.57	13.43
BLG14-2	0.88	11.30	72.20	2.84	18.15	14.14	90.35	79.89	20.11
BLG14-3	0.97	13.72	87.67	5.05	32.27	18.77	119.94	73.12	26.88
BLG14-4	1.09	13.67	87.35	6.86	43.83	20.53	131.18	66.60	33.40
BLG14-5	1.25	10.47	66.90	9.49	60.64	19.95	127.48	52.46	47.55
BLG14-6	1.53	5.36	34.25	7.79	49.78	13.15	84.03	40.78	59.22

<sup>a</sup>Percentage of retained oil ( $P_{RO}$ ): ratio of the retained oil yield to the total oil yield.

<sup>b</sup>Percentage of expelled oil ( $P_{EO}$ ): ratio of the expelled oil yield to the total oil yield.

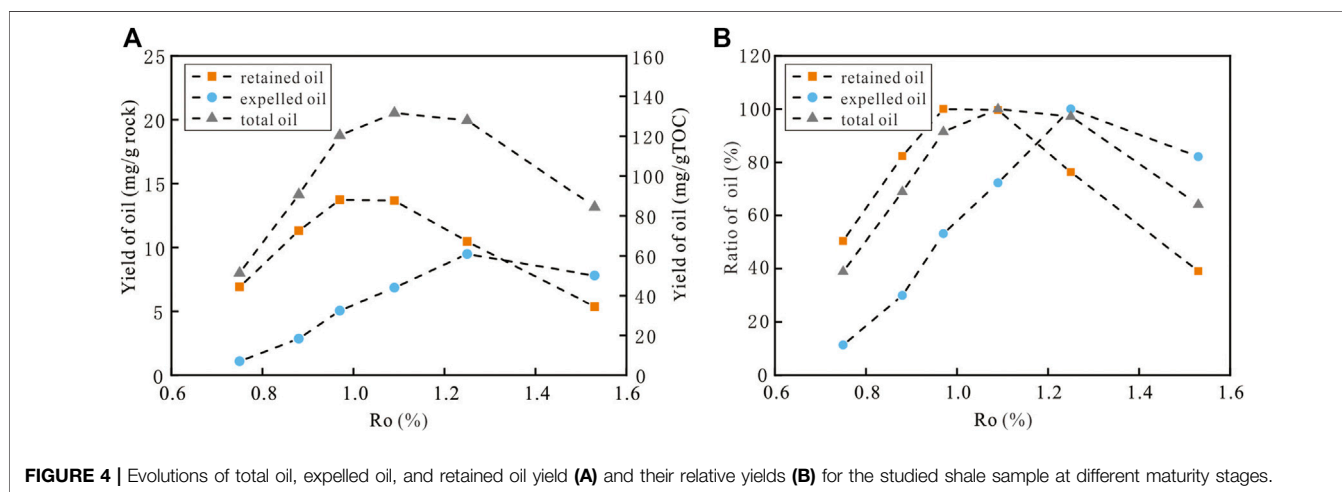
**FIGURE 4** | Evolutions of total oil, expelled oil, and retained oil yield (A) and their relative yields (B) for the studied shale sample at different maturity stages.

exhibit gray color under reflected light (Figure 2A–C), and it also contains abundant exinite (sporophore) and lamalginite, which exhibit dark and bright yellow colors, respectively, under fluorescence excitation (Figure 2D–F). These characteristics indicate that the organic matter of this shale came from both terrigenous higher organisms and aquatic alga, and the contribution of the former sources was greater than that of latter sources.

## Evolutions of Oil Generation and Expulsion

In this study, the  $R_o$  values of the artificially matured shale samples correspond well with experimental temperatures, and they exhibit a significant positive relationship (Figure 3). With the experimental temperature increasing from 350°C to 460°C, the  $R_o$  value increases from 0.75% to 1.53% (Table 2). The maturity range of artificially matured shales covers from the early oil generation stages to the wet gas stages.

The yields of the expelled oils ( $Y_{EO}$ ), retained oils ( $Y_{RO}$ ), and total generated oils ( $Y_{TO}$ ) are listed in Table 2, and the  $Y_{EO}$ ,  $Y_{RO}$ , and  $Y_{TO}$  exhibit different evolutions with the increasing maturity (Figure 4A). The  $Y_{EO}$  increases from 1.07 mg/g rock to the maximum yield of 9.49 mg/g rock with the  $R_o$  increasing from 0.75% to 1.25%. However, when the  $R_o > 1.25\%$ , the  $Y_{EO}$  gradually decreases to 7.79 mg/g rock as the  $R_o$  increases to 1.53% (Table 3 and Figure 4A). The  $Y_{RO}$  increases from

6.92 mg/g rock to the maximum yield of 13.72 mg/g rock with the  $R_o$  increasing from 0.75% to 0.97%. However, when the  $R_o > 0.97\%$ , the  $Y_{RO}$  gradually decreases to 5.36 mg/g rock as the  $R_o$  increases to 1.53% (Table 3 and Figure 4A). The  $Y_{TO}$  increases from 8.00 mg/g rock to the maximum yield of 20.53 mg/g rock with the  $R_o$  increasing from 0.75% to 1.09%, which indicates that the generation rates of oils are greater than their pyrolysis rates at this stage. However, when the  $R_o > 1.09\%$ , the  $Y_{TO}$  gradually decreases to 13.15 mg/g rock as the  $R_o$  increases to 1.53%, which indicates that the generation rates of oils are smaller than their pyrolysis rates at this stage (Table 2 and Figure 4A). The main oil generation and expulsion stages are generally defined in the range of 30%–80% of the maximum oil yield (Sun et al., 2019). According to this definition, the main stages of oil generation and expulsion are 0.85%–1.15% and 0.70%–0.95%, respectively, for the studied marine-terrestrial transitional shale sample. The main stages of oil expulsion are later than those of oil generation (Figure 4B).

Previous pyrolysis experiments performed on lacustrine shales with type I or type II kerogen indicate that these shales begin to generate oils when the  $R_o > 0.70\%$ , and the oil generation windows are in the  $R_o$  range of 0.75%–0.90% (Sun et al., 2019). The differences in oil generation stages of various shales are largely determined by their organic sources. For example, the oil generation thresholds of terrestrial organic

**TABLE 3** | Gross compositions of the expelled and retained oils at different maturity stages.

Sample number	$R_o$ (%)	Expelled oil (%)				Retained oil (%)			
		Saturates	Aromatics	Resins	Asphaltenes	Saturates	Aromatics	Resins	Asphaltenes
BLG14-1	0.75	7.27	18.18	5.45	69.09	1.93	8.82	11.30	77.96
BLG14-2	0.88	6.33	25.32	13.90	54.43	2.45	7.34	20.00	70.17
BLG14-3	0.97	9.79	20.28	20.30	49.65	3.87	9.61	22.40	64.11
BLG14-4	1.09	15.85	16.67	30.10	37.40	7.17	11.03	22.00	59.85
BLG14-5	1.25	18.75	17.75	31.80	31.75	14.30	16.93	27.80	40.94
BLG14-6	1.53	19.59	26.32	32.20	21.93	20.17	17.85	35.50	26.50

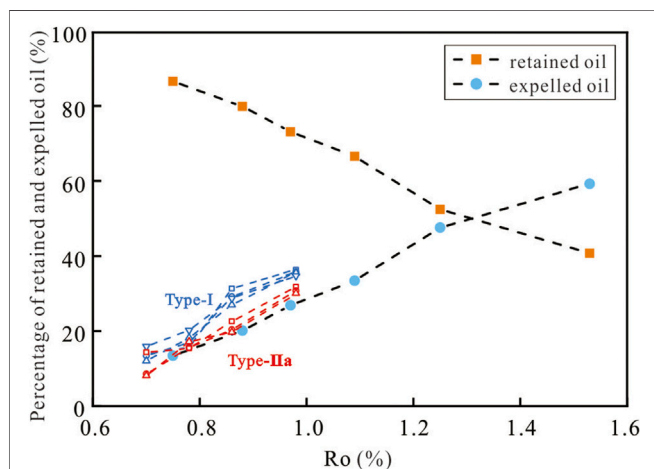


**FIGURE 5** | Relative percentages of the expelled ( $P_{EO}$ ) and retained oils ( $P_{RO}$ ) in total generated oils at different maturity stages for the studied marine-terrestrial transitional shale. The data of type I and II<sub>a</sub> lacustrine shales are cited from Sun et al. (2021).

matters, such as vitrinite and exinite, are generally at relative low maturity stages with  $R_o$  values of 0.50%–0.55%, and the main oil generation stages covered a wide maturity range with  $R_o$  values of 0.55%–1.00% (Li et al., 2002; Shuai et al., 2009). However, the oil generation threshold of aquatic alginates is generally at a higher maturity stage with the  $R_o$  value of 0.70%, and its main oil generation stage generally covers a shorter maturity range with  $R_o$  values of 0.70%–0.90%. In contrast to lacustrine shales, the studied marine-terrestrial transitional shale is richer in terrestrial organic matter, which results in an earlier oil generation threshold and a wider oil generation window.

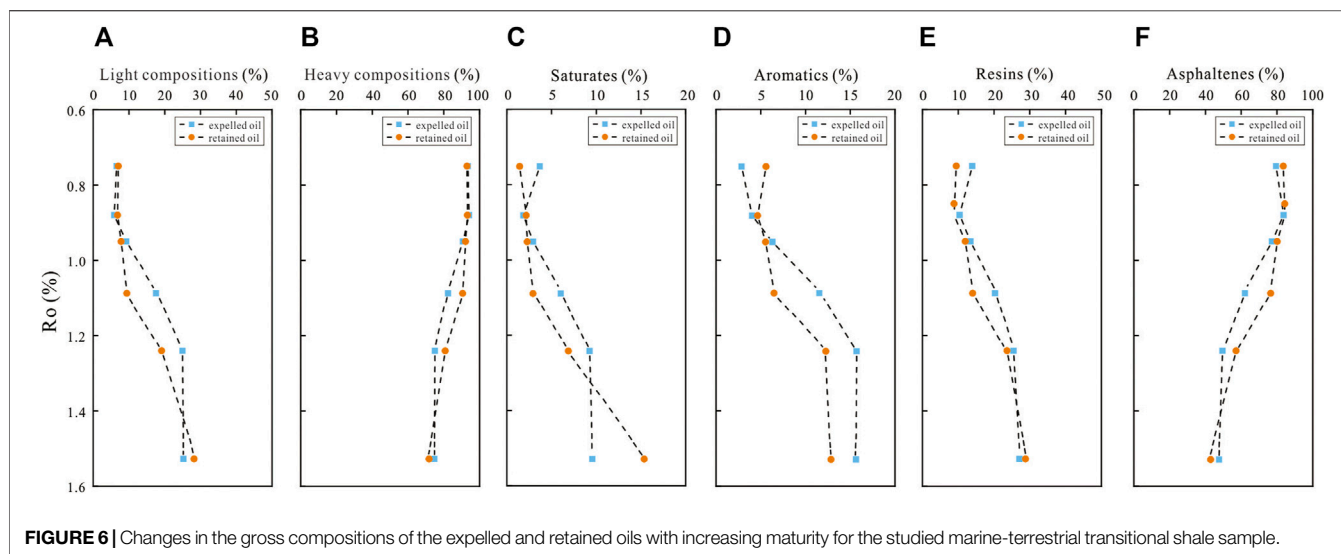
The relative percentages of expelled ( $P_{EO}$ ) and retained oils ( $P_{RO}$ ) in total generated oils obviously vary at different maturity stages (Figure 5). With the  $R_o$  increasing from 0.75 to 0.97%, the  $P_{EO}$  successively increases from 14% to 34%, while the  $P_{RO}$  progressively decreases from 86% to 67%. When the  $R_o$  values < 1.25%, the  $P_{RO}$  is higher than the  $P_{EO}$ ; however, the  $P_{RO}$  is lower than the  $P_{EO}$  when the  $R_o$  values > 1.25% (Figure 5). Heavy liquid hydrocarbons in the retained oils progressively cracked into light liquid hydrocarbons and promoted oil expulsions during the high maturity stages (Li et al., 2017). Shao et al. (2020) also reported that the peak  $P_{EO}$  value of Barnett lacustrine shales occurred in

the late wet gas stage with the  $R_o$  value of 1.75%. For the Shahejie Formation lacustrine shales in the Bohaiwan Basin (Sun et al., 2021), the shales with type I and II<sub>a</sub> kerogen generally have higher  $P_{EO}$  values than the shales with type II<sub>b</sub> and III kerogen (Figure 5). Under similar maturity conditions, the studied marine-terrestrial transitional shale has lower  $P_{EO}$  values than the lacustrine shales; however, its  $P_{EO}$  values significantly increase at high maturity stages, which indicates that oil expulsions are enhanced at high maturity stages for the studied shale.

The evolution model of oil generation and expulsion of the studied marine-terrestrial transitional shale is different from that of lacustrine shales reported by previous studies. Compared with the lacustrine shales, the marine-terrestrial transitional shales have earlier oil generation thresholds and wider oil generation windows. In addition, the  $P_{EO}$  values are similar for the two types of shales, while the  $P_{EO}$  values of marine-terrestrial transitional shales are significantly enhanced at high maturity stages. However, it should be pointed out that further studies need to be performed on more marine-terrestrial transitional shale samples to verify the applications of this oil generation and expulsion model under geological conditions.

## Changes in Gross Compositions of the Expelled and Retained Oils

The changes in gross compositions of the expelled and retained oils can be approximately divided into three stages. At the early stage with  $R_o$  < 0.97%, the gross compositions slightly changed with the maturity for both expelled and retained oils (Figure 6), which indicates that the fractionation effect caused by oil generation and expulsion is weak at this stage. At the middle stage with the  $R_o$  ranging from 0.97% to 1.25%, the light compositions (saturates and aromatics) obviously enriched while the heavy compositions (resins and asphaltenes) significantly decreased for both expelled and retained oils (Figure 6), because the kerogen generated more light compositions at this maturity stage. The percentages of the light compositions in expelled oils are significantly higher than those in retained oils (Figure 6), because the light compositions have low viscosity and tend to migrate (Pepper and Corvi, 1995). Therefore, a significant fractionation occurred between the expelled and retained oils at this maturity stage. At the late stage with  $R_o$  > 1.25%, only a small number of light compositions were generated from kerogen; meanwhile, part of the retained and expelled oils cracked into gaseous



hydrocarbons. Therefore, with the increasing maturity, the differences in gross compositions between the two types of oils gradually decrease.

It is noteworthy that heavy compositions, especially the asphaltenes, are dominated in both retained and expelled oils during the oil generation and expulsion processes. At the maturity stages with the  $R_o$  range from 0.75% to 0.97%, the percentages of asphaltene in the expelled and retained oils account for 50%–69% and 63%–77%, respectively. At the high maturity stage with  $R_o$  of 1.53%, the percentages of asphaltene in the two types of oils account for 54% and 62%, respectively (Table 3). The gross compositions of expelled and retained oils significantly differ from those of lacustrine shales. At the stages with  $R_o$  values of 0.71%–1.41%, the light compositions account for 50%–69% and 63%–77% for the Eocene Shahejie lacustrine shales in the Bohaiwan Basin, respectively; moreover, with the increasing maturity, the resin content decreases while the asphaltene content increases for the lacustrine shales (Sun et al., 2021). Asphaltenes are dominated in the retained and expelled oils of marine-terrestrial transitional shales because of their abundant terrestrial organic sources.

## Mechanisms of Oil Generation and Expulsion

Ungerer et al. (1990) proposed that hydrocarbon generations from kerogen pyrolysis were mainly through two approaches, i.e., the depolymerization and functional group desorption. The former refers to the idea that kerogen initially cracks to intermediate products (resin and asphaltene), and then these intermediate products are further decomposed to oils and gases. The latter refers to the notion that functional groups initially bonded in kerogen skeletons can be directly liberated from the kerogen and form hydrocarbons. In this study, the  $Y_{TO}$  exhibits obvious positive correlations with the resin yield ( $Y_R$ ) and its percentage during the main oil generation and expulsion stages

(Figures 7A,B). The  $Y_{TO}$  is positively correlated with the asphaltenes yield ( $Y_A$ ) and its percentage when the  $R_o < 1.09\%$ , while it shows no obvious correlations with the  $Y_A$  and its percentage when  $R_o > 1.09\%$  (Figures 7C,D). Combined with the gross compositions and their evolutions of the expelled and retained oils (Figure 6), this study indicates that the organic matter of this studied marine-terrestrial transitional shale first depolymerized to asphaltenes at the early stages of oil generation, and then the transitional asphaltenes were further cracked into hydrocarbons at the late stages of oil generation, while the organic matter of lacustrine shales generates hydrocarbons mainly *via* transitional resins (Sun et al., 2021). Therefore, shales with different sedimentary facies are diverse in oil generation mechanism.

The oil generation and expulsion of shales are mainly controlled by their geochemical properties, including TOC content, kerogen type, maturity, and mineral compositions (Pepper and Corvi, 1995; Chen et al., 2014; Liang et al., 2015), and by their geological conditions, including geological temperature and pressure, water-bearing characteristic, strata thickness, and its boundary condition (Lewan 1997; Chen and Cha, 2005). Previous studies indicated that the pore systems of shales were fully adsorbed and filled by generated oils before oil expulsions, and kerogen swelling effects were the controlling factor on the oil retention in shale reservoirs (Li et al., 2016; Han et al., 2017; Ziegs et al., 2017; Shao et al., 2018). This study further shows that the marine-terrestrial transitional shale exhibits obvious oil expulsion under experimental conditions. Under similar maturity and kerogen-type conditions, marine-terrestrial transitional shales have similar  $P_{EO}$  values with lacustrine shales. The high  $P_{EO}$  values of the studied marine-terrestrial transitional shale can be illustrated by the following factors.

The kerogen swelling effect is closely related to kerogen types, and it decreases in the order of type I, type II<sub>a</sub>, and type II<sub>b</sub> kerogen. For example, the swelling amounts of type I, II<sub>a</sub>, and II<sub>b</sub>

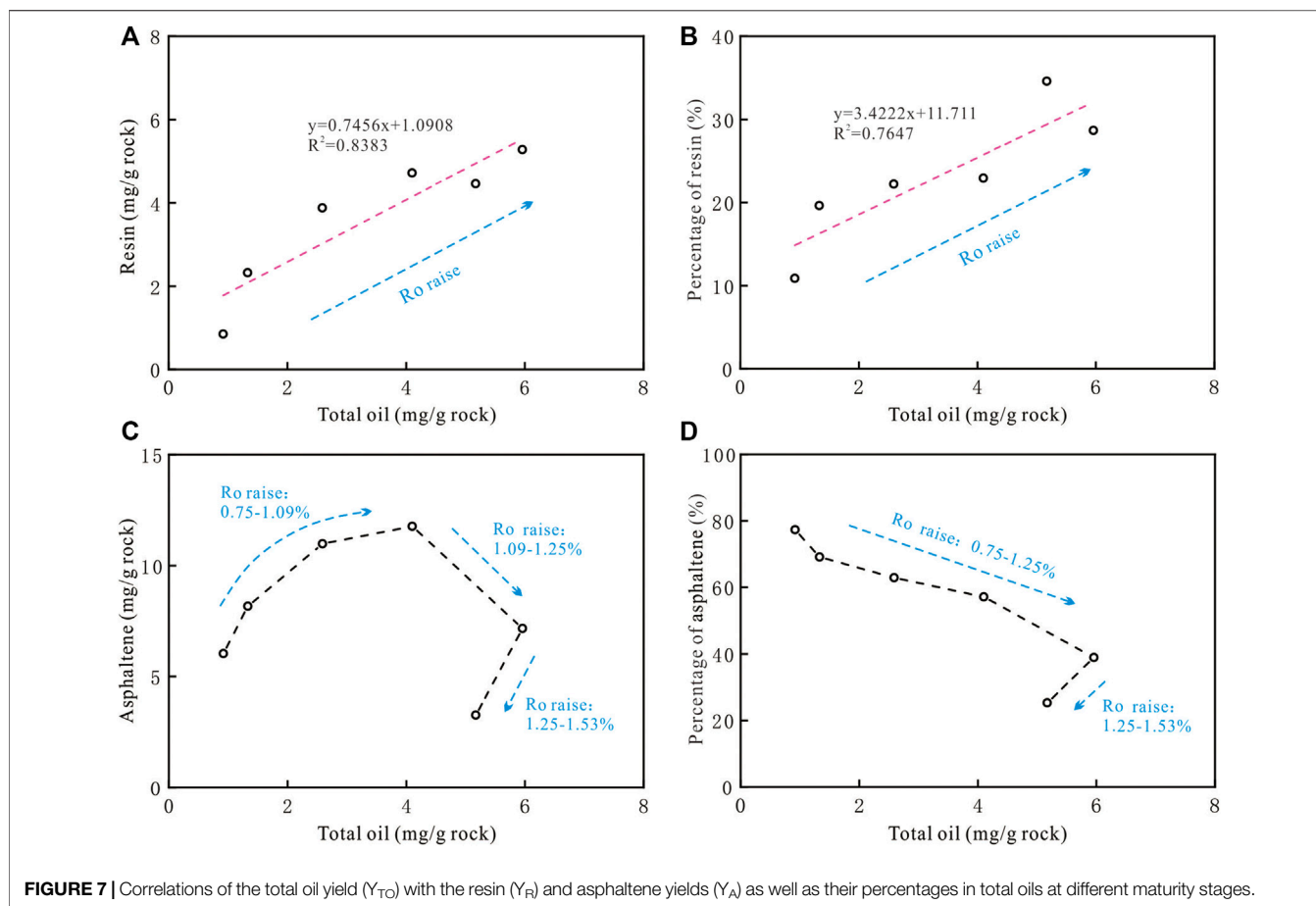


**FIGURE 7** | Correlations of the total oil yield ( $Y_{TO}$ ) with the resin ( $Y_R$ ) and asphaltene yields ( $Y_A$ ) as well as their percentages in total oils at different maturity stages.

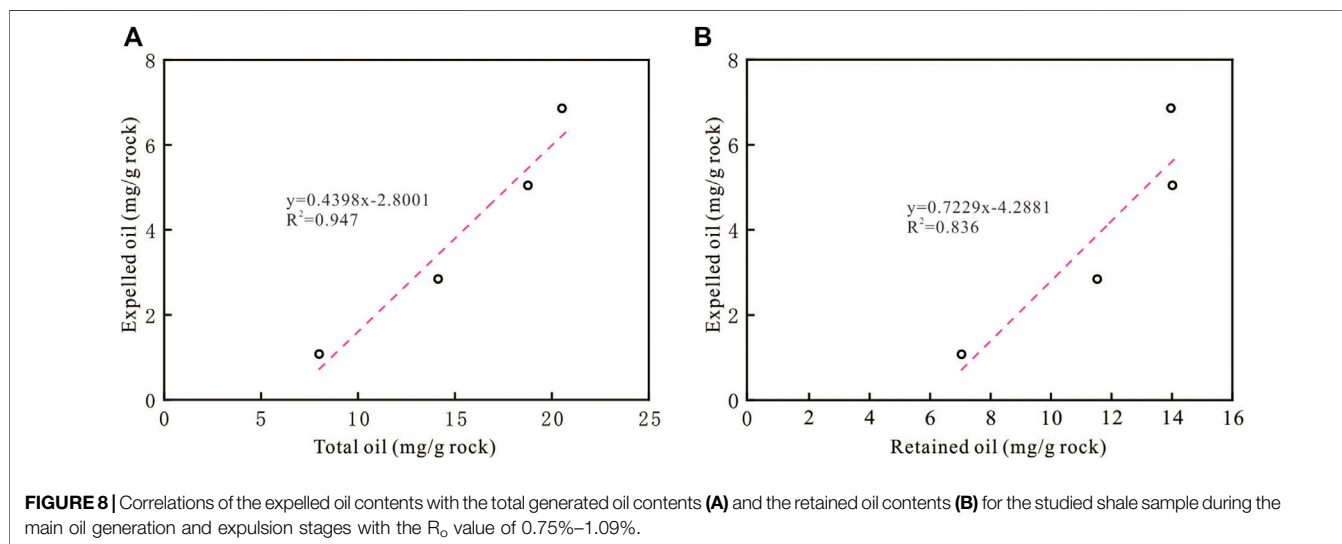


**FIGURE 8** | Correlations of the expelled oil contents with the total generated oil contents **(A)** and the retained oil contents **(B)** for the studied shale sample during the main oil generation and expulsion stages with the  $R_o$  value of 0.75%–1.09%.

kerogen, with a low maturity of 0.5%, are 142 mg/g TOC, 119 mg/g TOC, and 95 mg/g TOC, respectively (Tian et al., 2014). According to the intercept of the linear correlation equations in **Figure 8**, this study further estimated that the oil expulsion threshold of the studied marine-terrestrial transitional shale

corresponded to the  $Y_{TO}$  value of 6.4 mg/g rock and the  $Y_{RO}$  value of 5.9 mg/g rock. The maximum  $Y_{RO}$  value of this shale is 88 mg/g TOC (**Figure 4**) and is much lower than the maximum  $Y_{RO}$  values of the type I and type II<sub>a</sub> lacustrine shales, with values of 300–350 mg/g TOC and 150–200 mg/g TOC, respectively (Sun



et al., 2021). Although some retained oils are stored in inorganic-hosted nanopores of minerals, most of the retained oils are associated with the kerogen swelling effect (Li et al., 2016; Zhao et al., 2019). The studied marine-terrestrial transitional shale with type II<sub>b</sub> kerogen has a low capacity of retaining oils resulting from its weak kerogen swelling effect, which may be the main mechanism for its high oil expulsion efficiency.

Under geological conditions, shale reservoirs generally contain some pore waters that significantly influence the accumulation and enrichment of shale oil and gas resources (Lewan 1997; Burnham 1998; Carr et al., 2009; Lewan and Roy, 2011; Cheng et al., 2018). The pore waters not only take up the pore spaces available for oil storage, but also occupy pore surfaces and change the interfaces between hydrocarbons and pore walls, which significantly prompts oil migrations and expulsions (Korb et al., 2014; Ma et al., 2015; Cheng et al., 2017; Zolfaghari et al., 2017). Moreover, pore waters may also cause an overpressure in shale pore systems, and thus enhance the oil expulsion efficiency (Zhang et al., 2011; Huang et al., 2017). In addition, since the oil expulsion efficiency is positively correlated with the TOC content (Zhang et al., 2006; Sun et al., 2021), the high TOC content of the studied shale sample may also raise its oil expulsion efficiency.

At present, the oil generation and expulsion model of marine-terrestrial transitional shale remains unclear. The results of this study show that oil expulsions of marine-terrestrial transitional shales with high TOC contents may occur under geological conditions, and the oil expulsion efficiency and the geochemical properties of expelled and retained oils are largely determined by the organic sources and maturities of shales. The new understanding on the oil generation and expulsion model in this study may have a certain theoretical significance for the exploration and development of marine-terrestrial transitional shale resources. However, the oil generation and expulsion model of marine-terrestrial transitional shales with type III kerogen needs to be investigated in further studies.

## CONCLUSION

In this study, a pyrolysis experiment was performed on water-saturated marine-terrestrial transitional shale plunger samples, to simulate the evolutions of oil generation and expulsion. The main conclusions are as follows:

- 1) In contrast to marine and lacustrine shales, marine-terrestrial transitional shales have wider maturity ranges of oil generation and expulsion, and the main stages of oil expulsion are later than those of oil generation, with corresponding  $R_o$  values of 0.85%–1.15% and 0.70%–0.95%, respectively.

## REFERENCES

Burnham, A. K. (1998). Comment on "Experiments on the Role of Water in Petroleum Formation" by M.D. Lewan. *Geochim. Cosmochim. Acta* 62 (12), 2207–2210.

- 2) The expelled and retained oils of marine-terrestrial transitional shales exhibit obvious fractionations in compositions during the oil generation and expulsion process. However, the two types of oils are dominated by heavy compositions, which significantly differs from the generated oils from marine and lacustrine shales.
- 3) The oil generation and expulsion evolutions of marine-terrestrial transitional shales are largely determined by their organic sources of terrigenous higher organisms. The kerogen of these shales initially depolymerized to transitional asphaltenes, which further cracked into hydrocarbons, and the weak swelling effects of the kerogen promoted oil expulsions.

## DATA AVAILABILITY STATEMENT

The original contributions presented in the study are included in the article/Supplementary Material, Further inquiries can be directed to the corresponding authors.

## AUTHOR CONTRIBUTIONS

QF: Conceptualization, Methodology, Data curation, Writing - Original Draft. PC: Conceptualization, Methodology, Review and Editing. XX: Supervision, Review and Editing. HG: Methodology and Review. QZ: Investigation and Editing. TL: Review and Editing. PG: Review and Editing. All authors listed have made a substantial, direct, and intellectual contribution to the work and approved it for publication.

## FUNDING

This study was supported by the National Natural Science Foundation of China (U1810201, 41402116, and 42173031), the Natural Science Foundation of Guangdong Province (2021A1515011381), and the Independent Project of the SKLOG (2020–2). The experimental data in this study were measured in the Experimental Platform of Organic Geochemistry, the Public Technical Service Center of Guangzhou Institute of Geochemistry, CAS.

## ACKNOWLEDGMENTS

We are indebted to Prof. Zhang Kaijun and Huang Qiangtai as well as two reviewers for their insightful comments and suggestions that have greatly improved the manuscript.

Cao, Y., Han, H., Liu, H.-w., Jia, J.-c., Zhang, W., Liu, P.-w., et al. (2019). Influence of Solvents on Pore Structure and Methane Adsorption Capacity of Lacustrine Shales: An Example from a Chang 7 Shale Sample in the Ordos Basin, China. *J. Pet. Sci. Eng.* 178, 419–428. doi:10.1016/j.petrol.2019.03.052

Carr, A. D., Snape, C. E., Meredith, W., Uguna, C., Scotchman, I. C., and Davis, R. C. (2009). The Effect of Water Pressure on Hydrocarbon Generation Reactions:

- Some Inferences from Laboratory Experiments. *Pet. Geosci.* 15 (1), 17–26. doi:10.1144/1354-079309-797
- Chalmers, G. R. L., and Bustin, R. M. (2008). Lower Cretaceous Gas Shales in Northeastern British Columbia, Part I: Geological Controls on Methane Sorption Capacity. *Bull. Can. Pet. Geology.* 56 (1), 1–21. doi:10.2113/gscpgbull.56.1.1
- Chen, Z. H., and Cha, M. (2005). Geochemical Characteristics of Source Rocks in Dongying Depression. *Geochimica* 34 (01), 79–87. doi:10.19700/j.0379-1726.2005.01.010
- Chen, D., Huang, X. H., Li, L. T., Deng, K., Zheng, J. H., and Hong, Q. (2010). Characteristics and History of Hydrocarbon Expulsion of the Upper Tertiary Source Rocks in the Western Sichuan Depression. *Nat. Gas Industry* 30 (05), 41–45. doi:10.3787/j.issn.1000-0976.2010.05.010
- Chen, J. P., Sun, Y. G., Zhong, N. N., Huang, Z. K., Deng, C. P., Xie, L. J., et al. (2014). The Efficiency and Model of Petroleum Expulsion from the Lacustrine Source Rocks within Geological Frame. *Acta Geol. Sin.* 88 (11), 2005–2032. doi:10.1111/1755-6724.12373\_3
- Cheng, P., Tian, H., Xiao, X., Gai, H., Li, T., and Wang, X. (2017). Water Distribution in Overmature Organic-Rich Shales: Implications from Water Adsorption Experiments. *Energy Fuels* 31, 13120–13132. doi:10.1021/acs.energyfuels.7b01531
- Cheng, P., Xiao, X., Tian, H., and Wang, X. (2018). Water Content and Equilibrium Saturation and Their Influencing Factors of the Lower Paleozoic Overmature Organic-Rich Shales in the Upper Yangtze Region of Southern China. *Energy Fuels* 32, 11452–11466. doi:10.1021/acs.energyfuels.8b03011
- Cheng, P., Xiao, X., Wang, X., Sun, J., and Wei, Q. (2019). Evolution of Water Content in Organic-Rich Shales with Increasing Maturity and its Controlling Factors: Implications from a Pyrolysis experiment on a Water-Saturated Shale Core Sample. *Mar. Pet. Geol.* 109, 291–303. doi:10.1016/j.marpetgeo.2019.06.023
- Gai, H., Xiao, X., Cheng, P., Tian, H., and Fu, J. (2015). Gas Generation of Shale Organic Matter with Different Contents of Residual Oil Based on a Pyrolysis experiment. *Org. Geochem.* 78, 69–78. doi:10.1016/j.orggeochem.2014.11.001
- Guo, S. B., Fu, J. J., Gao, D., and Li, H. Y. (2015). Research Status and Prospects for marine-continental Shale Gases in China. *Pet. Geol. Exp.* 37 (05), 535–540. doi:10.11781/syysdz201505535
- Guo, S. B., Wang, Z. L., and Xiao, M. (2021). Exploration prospect of Shale Gas with Permian Transitional Facies of Some Key Areas in China. *Pet. Geol. Exp.* 43 (03), 377–385. doi:10.11781/syysdz202103377
- Hakimi, M. H., Alauga, A. S., Ahmed, A. F., Yahya, M. M. A., El Nady, M. M., and Ismail, I. M. (2018). Simulating the Timing of Petroleum Generation and Expulsion from Deltaic Source Rocks: Implications for Late Cretaceous Petroleum System in the Offshore Jiza-Qamar Basin, Eastern Yemen. *J. Pet. Sci. Eng.* 170, 620–642. doi:10.1016/j.petrol.2018.06.076
- Han, Y., Mahlstedt, N., and Horsfield, B. (2015). The Barnett Shale: Compositional Fractionation Associated with Intraformational Petroleum Migration, Retention, and Expulsion. *Bulletin* 99 (12), 2173–2202. doi:10.1306/06231514113
- Han, Y., Horsfield, B., Wirth, R., Mahlstedt, N., and Bernard, S. (2017). Oil Retention and Porosity Evolution in Organic-Rich Shales. *Bulletin* 101 (6), 807–827. doi:10.1306/09221616069
- Huang, H., Chen, S., Lu, J., Ma, J., and He, J. (2017). The Influence of Water on the thermal Simulation experiment of Hydrocarbon Generation and Expulsion. *Pet. Sci. Technol.* 35 (8), 783–788. doi:10.1080/10916466.2016.1277239
- Huang, D., Yang, G., Yang, Z., Yang, T. Q., Bai, R., and Li, Y. C. (2019). New Understanding and Development Potential of Tight Oil Exploration and Development in Sichuan Basin. *Nat. Gas Geosci.* 30 (08), 1212–1221. doi:10.11764/j.issn.1672-1926.2019.07.005
- Inan, S., and Schenk, H. J. (2001). Evaluation of Petroleum Generation and Expulsion from a Source Rock by Open and Restricted System Pyrolysis Experiments. Part I. Extrapolation of Experimentally-Derived Kinetic Parameters to Natural Systems. *J. Anal. Appl. Pyrolysis* 58, 213–228. doi:10.1016/S0165-2370(00)00188-1
- Jin, Z. J., Bai, Z. R., Gao, B., and Li, M. W. (2019). Has China Ushered in the Shale Oil and Gas Revolution? *Oil Gas Geol.* 40 (03), 451–458. doi:10.11743/ogg20190301
- Ko, L. T., Ruppel, S. C., Loucks, R. G., Hackley, P. C., Zhang, T., and Shao, D. (2018). Pore-types and Pore-Network Evolution in Upper Devonian-Lower Mississippian Woodford and Mississippian Barnett Mudstones: Insights from Laboratory thermal Maturation and Organic Petrology. *Int. J. Coal Geol.* 190, 3–28. doi:10.1016/j.coal.2017.10.001
- Korb, J.-P., Nicot, B., Louis-Joseph, A., Bubici, S., and Ferrante, G. (2014). Dynamics and Wettability of Oil and Water in Oil Shales. *J. Phys. Chem. C* 118 (40), 23212–23218. doi:10.1021/jp508659e
- Lewan, M. D., and Roy, S. (2011). Role of Water in Hydrocarbon Generation from Type-I Kerogen in Mahogany Oil Shale of the Green River Formation. *Org. Geochem.* 42 (1), 31–41. doi:10.1016/j.orggeochem.2010.10.004
- Lewan, M. D., Winters, J. C., and McDonald, J. H. (1979). Generation of Oil-Like Pyrolyzates from Organic-Rich Shales. *Science* 203 (4383), 897–899. doi:10.1126/science.203.4383.897
- Lewan, M. D. (1997). Experiments on the Role of Water in Petroleum Formation. *Geochim. Cosmochim. Acta* 61 (17), 3691–3723. doi:10.1016/S0016-7037(97)00176-2
- Li, X. Q., Xiong, B., Ma, A. L., Wang, F. Y., and Zhong, N. N. (2002). Advance of Organic Petrology in Oil and Gas Exploration. *J. Jiangnan Pet. Inst.* 24 (01), 15–19. doi:10.3969/j.issn.1000-9752.2002.01.005
- Li, Z., Zou, Y.-R., Xu, X.-Y., Sun, J.-N., Li, M., and Peng, P. A. (2016). Adsorption of Mudstone Source Rock for Shale Oil - Experiments, Model and a Case Study. *Org. Geochem.* 92, 55–62. doi:10.1016/j.orggeochem.2015.12.009
- Li, Z. M., Rui, X. Q., Xu, E. S., Yang, Z. H., and Ma, Z. L. (2017). Simulation of Hydrocarbon Generation and Expulsion for Brown Coal with Transitional Organic Matter Type II<sub>2</sub>-III under Near Geological Conditions. *J. China Coal Soc.* 42 (01), 249–256. doi:10.13225/j.cnki.jccs.2016.0566
- Liang, M., Wang, Z., Zheng, J., Li, X., Wang, X., Gao, Z., et al. (2015). Hydrous Pyrolysis of Different Kerogen Types of Source Rock at High Temperature-Bulk Results and Biomarkers. *J. Pet. Sci. Eng.* 125, 209–217. doi:10.1016/j.petrol.2014.11.021
- Liu, D. H., Fu, J. M., Xiao, X. M., Chen, D. Y., and Geng, A. S. (2005). Origin and Appraisal of Coal Derived Gas and Oil. *Pet. Exploration Dev.* 32 (04), 137–141. doi:10.3321/j.issn:1000-0747.2005.04.023
- Ma, Z. L., Zheng, L. J., Zhao, Z. X., and Ge, Y. (2015). Effect of Fluid Medium in Source Rock Porosity on Oil Primary Migration. *Pet. Geology. Exp.* 37 (01), 97–101. doi:10.7603/s40972-015-0016-4
- Mao, R., Mi, J. K., and Zhang, S. C. (2012). Study on the Hydrocarbon Generation Characteristics of Different Coaly Source Rocks by Gold-Tube Pyrolysis Experiments. *Nat. Gas Geosci.* 23 (06), 1127–1134. doi:10.11764/j.issn.1672-1926.2012.06.021
- Pepper, A. S., and Corvi, P. J. (1995). Simple Kinetic Models of Petroleum Formation. Part III: Modelling an Open System. *Mar. Pet. Geol.* 12 (4), 417–452. doi:10.1016/0264-8172(95)96904-5
- Qin, Y., Shen, J., and Shen, Y. L. (2016). Joint Mining Compatibility of Superposed Gas-Bearing Systems: A General Geological Problem Extraction of Three Natural Gases and Deep CBM in Coal Series. *J. China Coal Soc.* 41 (01), 14–23. doi:10.13225/j.cnki.jccs.2015.9032
- Shao, X., Pang, X., Li, H., Hu, T., Xu, T., Xu, Y., et al. (2018). Pore Network Characteristics of Lacustrine Shales in the Dongpu Depression, Bohai Bay Basin, China, with Implications for Oil Retention. *Mar. Pet. Geol.* 96, 457–473. doi:10.1016/j.marpetgeo.2018.06.015
- Shao, D., Zhang, T., Ko, L. T., Li, Y., Yan, J., Zhang, L., et al. (2020). Experimental Investigation of Oil Generation, Retention, and Expulsion within Type II Kerogen-Dominated marine Shales: Insights from Gold-Tube Nonhydrous Pyrolysis of Barnett and Woodford Shales Using Miniature Core Plugs. *Int. J. Coal Geology.* 217, 103337. doi:10.1016/j.coal.2019.103337
- Shuai, Y. H., Zhang, S. C., and Chen, J. P. (2009). Comparison of the Oil Potential of Coal and Coaly Mudstone. *Geochimica* 38 (6), 583–590. doi:10.19700/j.0379-1726.2009.06.008
- Su, X., Lin, X., Zhao, M., Song, Y., and Liu, S. (2005). The Upper Paleozoic Coalbed Methane System in the Qinshui basin, China. *Bulletin* 89 (1), 81–100. doi:10.1306/07300403125
- Su, Y. F., Zhang, Q. H., Qu, X. R., and Wei, Z. C. (2016). Geological Evaluation of marine-continental Transitional-Facies Shale Gas and Optimal Selection of Favorable Areas, Shanxi Province. *Nat. Gas Explor. Dev.* 39 (03), 1–5. doi:10.3969/j.issn.1673-3177.2016.03.001
- Sun, L. N., Zhang, M. F., Wu, C. J., Xiong, D. M., and Su, L. (2015). The Effect of Water Medium on the Products of Different Pyrolysis System. *Nat. Gas Geosci.* 26 (03), 524–532. doi:10.1007/s12209-015-2667-6

- Sun, J., Xiao, X., Cheng, P., and Tian, H. (2019). Formation and Evolution of Nanopores in Shales and its Impact on Retained Oil during Oil Generation and Expulsion Based on Pyrolysis Experiments. *J. Pet. Sci. Eng.* 176, 509–520. doi:10.1016/j.petrol.2019.01.071
- Sun, J., Xiao, X., Cheng, P., Wang, M., and Tian, H. (2021). The Relationship between Oil Generation, Expulsion and Retention of Lacustrine Shales: Based on Pyrolysis Simulation Experiments. *J. Pet. Sci. Eng.* 196, 107625. ARTN 107625. doi:10.1016/j.petrol.2020.107625
- Tang, Y., Huang, Y., Ellis, G. S., Wang, Y., Kralert, P. G., Gillaizeau, B., et al. (2005). A Kinetic Model for Thermally Induced Hydrogen and Carbon Isotope Fractionation of Individual N-Alkanes in Crude Oil. *Geochim. Cosmochim. Acta* 69 (18), 4505–4520. doi:10.1016/j.gca.2004.12.026
- Tang, X., Zhang, J., Jiang, Z., Zhao, X., Liu, K., Zhang, R., et al. (2015). Characteristics of Solid Residue, Expelled and Retained Hydrocarbons of Lacustrine Marlstone Based on Semi-closed System Hydrous Pyrolysis: Implications for Tight Oil Exploration. *Fuel* 162, 186–193. doi:10.1016/j.fuel.2015.09.009
- Tian, H., Xiao, X., Wilkins, R. W. T., and Tang, Y. (2012). An Experimental Comparison of Gas Generation from Three Oil Fractions: Implications for the Chemical and Stable Carbon Isotopic Signatures of Oil Cracking Gas. *Org. Geochem.* 46, 96–112. doi:10.1016/j.orggeochem.2012.01.013
- Tian, S. S., Xue, H. T., and Lu, S. F. (2014). “Discussion on the Mechanism of Different Types of Kerogen Remaining Oil and Gas,” in 2014 Annual Meeting of Chinese Geoscience Union (Beijing: Annual Meeting of Chinese Geoscience Union), 2509–2512.
- Ungerer, P., Burrus, J., Doligez, B., Chenet, P. Y., and Bessis, F. (1990). Basin Evaluation by Integrated 2-dimensional Modeling of Heat-Transfer, Fluid-Flow, Hydrocarbon Generation, and Migration. *AAPG Bull.-Am. Assoc. Pet. Geol.* 74 (3), 309–335. doi:10.1306/0c9b22db-1710-11d7-8645000102c1865d
- van Krevelen, D. W. (1961). *Coal: Typology-Chemistry-Physics-Constitution*. Amsterdam: Elsevier, 514.
- Wei, Z., Zou, Y.-R., Cai, Y., Wang, L., Luo, X., and Peng, P. A. (2012). Kinetics of Oil Group-type Generation and Expulsion: An Integrated Application to Dongying Depression, Bohai Bay Basin, China. *Org. Geochem.* 52, 1–12. doi:10.1016/j.orggeochem.2012.08.006
- Wu, X. Q., Wang, P., Liu, Q. Y., Li, H. J., Chen, Y. B., and Zeng, H. H. (2016). The Source of Natural Gas Reservoir in the 5th Member of the Upper Triassic Xujiahe Formation in Xinchang Gasfield, The Western Sichuan Depression and its Implication. *Nat. Gas Geosci.* 27 (08), 1409–1418. doi:10.11764/j.issn.1672-1926.2016.08.1409
- Wu, Y., Zhang, Z., Sun, L., Li, Y., Su, L., Li, X., et al. (2018). The Effect of Pressure and Hydrocarbon Expulsion on Hydrocarbon Generation during Pyrolyzing of continental Type-III Kerogen Source Rocks. *J. Pet. Sci. Eng.* 170, 958–966. doi:10.1016/j.petrol.2018.06.067
- Zhang, W. Z., Yang, H., and Li, J. F. (2006). Leading Effect of High-Class Source Rock of Chang 7 in Ordos Basin on Enrichment of Low Permeability Oil-Gas Accumulation. *Pet. Explor. Dev.* 33 (03), 289–293. doi:10.3321/j.issn:1000-0747.2006.03.006
- Zhang, L. J., He, S., Qian, J. Z., and Ma, Z. L. (2011). Formation Water of Near-Critical Properties and its Effects on the Processes of Hydrocarbon Generation and Expulsion. *Earth Sci.* 36 (01), 83–92. doi:10.3799/dqkx.2011.009
- Zhao, W. Z., Hu, S. Y., Hou, L. H., Yang, T., Li, X., and Guo, B. C. (2020). Types and Resource Potential of continental Shale Oil in China and its Boundary with Tight Oil. *Pet. Explor. Dev.* 47 (01), 1–10. doi:10.1016/s1876-3804(20)60001-5
- Zhao, X. Z., Zhou, L. H., Pu, X. G., Jin, F. M., and Shi, Z. N. (2019). Favorable Formation Conditions and Enrichment Characteristics of Lacustrine Facies Shale Oil in Faulted lake basin: a Case Study of Member 2 of Kongdian Formation in Cangdong Sag, Bohai Bay Basin. *Acta Petrolei Sin.* 40 (09), 1013–1029. doi:10.7623/syxb201909001
- Zhou, Q. F., Jin, Z. J., Yang, G. F., and Dong, N. (2019). Shale Oil Exploration and Production in the U.S.: Status and Outlook. *Oil Gas Geol.* 40 (03), 469–477. doi:10.11743/ogg20190303
- Ziegls, V., Horsfield, B., Skeie, J. E., and Rinna, J. (2017). Petroleum Retention in the Mandal Formation, Central Graben, Norway. *Mar. Pet. Geol.* 83, 195–214. doi:10.1016/j.marpetgeo.2017.03.005
- Zolfaghari, A., Dehghanpour, H., and Holyk, J. (2017). Water Sorption Behaviour of Gas Shales: I. Role of Clays. *Int. J. Coal Geol.* 179, 130–138. doi:10.1016/j.coal.2017.05.008
- Zou, C. N., Du, J. H., Xu, C. C., Wang, Z. C., Zhang, B. M., Wei, G. Q., et al. (2014). Formation, Distribution, Resource Potential and Discovery of the Sinian-Cambrian Giant Gas Field, Sichuan Basin, SW China. *Pet. Explor. Dev.* 41 (03), 278–293. doi:10.1016/s1876-3804(14)60036-7
- Zou, C. N., Yang, Z., Huang, S. P., Ma, F., Sun, Q. P., and Li, F. F. (2019). Resource Types, Formation, Distribution and Prospects of Coal-Measure Gas. *Pet. Explor. Dev.* 46 (03), 433–442. doi:10.1016/s1876-3804(19)60026-1
- Zou, C. N., Pan, S. Q. i., Jiang, Z. H., Gao, J. L., Yang, Z., and Wu, S. T. (2020). Shale Oil Anf Gas Revolution and its Impact. *Acta Petrolei Sin.* 41 (01), 1–12. doi:10.7623/syxb202001001

**Conflict of Interest:** The authors declare that the research was conducted in the absence of any commercial or financial relationships that could be construed as a potential conflict of interest.

**Publisher’s Note:** All claims expressed in this article are solely those of the authors and do not necessarily represent those of their affiliated organizations, or those of the publisher, the editors, and the reviewers. Any product that may be evaluated in this article, or claim that may be made by its manufacturer, is not guaranteed or endorsed by the publisher.

Copyright © 2021 Fan, Cheng, Xiao, Gai, Zhou, Li and Gao. This is an open-access article distributed under the terms of the Creative Commons Attribution License (CC BY). The use, distribution or reproduction in other forums is permitted, provided the original author(s) and the copyright owner(s) are credited and that the original publication in this journal is cited, in accordance with accepted academic practice. No use, distribution or reproduction is permitted which does not comply with these terms.